Site selection for new PV power plants based on their observability

L. Alfredo Fernandez-Jimenez, Montserrat Mendoza-Villena*, Pedro Zorzano-Santamaria, Eduardo Garcia-Garrido, Pedro Lara-Santillan, Enrique Zorzano-Alba, Alberto Falces
Department of Electrical Engineering, University of La Rioja, Luis de Ulloa 20, 26004 Logroño, Spain
*Corresponding author: Tel: +34941299490
E-mail address: montserrat.mendoza@unirioja.es

Abstract: Despite the advantages that power plants based on renewable energies offer, there are some restrictions to the social acceptance of these facilities. One of these restrictions is the visual impact that large power plants may generate on people. This paper presents a new methodology for ranking the feasible places in a zone for the construction of new photovoltaic (PV) power plants according to their visibility. The methodology is based on the fuzzy viewshed and the distance decay methods, which enable to calculate the maximum number of hours in a mean day in which the new PV plant may be viewed by each possible observer. This number is related to the inhabitants in the zone, the size of the plant, the possible observers from paths and roads, and their distance to the PV plant. The proposed methodology is implemented in a Geographical Information System which allows the presentation of visual results that help to identify the best areas in the zone under study. This methodology can be useful to local authorities who have to authorize the installation of the new power plant in the territory under their competence, or investors who are trying to find the best locations from the point of view of visual impact.

Keywords: Visual impact, PV plants, Geographic Information System, Site selection.

1. Introduction

A photovoltaic system is the most direct way to convert solar radiation into electricity. PV systems offer an alternative to traditional generation systems for low power applications in isolated areas and, in zones with access to electricity networks, can be connected to medium and low voltages grids. The expansion of grid-connected PV systems, as well as other renewable energy based plants, has experienced an important boost in recent years, in part due to help from policies implemented by national governments that establish capacity goals and promote them with feed-in tariff schemes and subsidies [1]. In the near future, PV energy production will become competitive at utility-scale with wholesale electricity prices in some world regions [2, 3], which will contribute to an increase in the construction of new large-scale PV plants.

The criteria used in site selection for new solar PV grid-connected plants can include: energy production, orography (slopes and orientation), environment (land use and visual impact), distances (to roads, to power substations, and to urban areas), financial, and climate (irradiance, temperature, etc.) [4, 5]. Although PV systems provide some advantages, as do most renewable energy based power plants, there are some restrictions with regard to the social acceptance of these facilities [6, 7]. One of these restrictions is the visual impact that large power plants causing undesired changes of the landscape may generate on people. The opposition of the local population can slow down and even block the construction of new power plants [8], so the selection of the places with lowest visual impact in a zone can contribute to an acceleration in their construction.

Visual impact assessment (VIA) has become an important issue in the development of projects for new wind farms [9-13]. Hurtado et al. [10] propose a scale with 6 levels, from minimum to deep, to evaluate the visual impact: the level is calculated taking into account the distance and the number of permanent inhabitants in the zone; the same methodology is refined by Tsoutsos et al. [11] and applied to a case study in Greece. The height and visibility of large wind turbines can make these power plants negatively affect the visual perception of the landscape. In general, visual impact assessment takes into account the distance from the observer to the wind farm. So, Molina-Ruiz et al. [12] consider the visual impact as high when the distance is less than 10 km; as intermediate when the distance ranges from 10 km to 20 km; and as low when the distance is greater. Additionally, Torres Sibille et al. [13] present a function for the calculation of an indicator of the objective aesthetic impact of wind farms: the factors used include visibility, fractality, colour, climatology and continuity of the wind turbines; the function is applied to two wind farms, in Spain and Wales, and the results are compared with those obtained by means of surveys with photographs among inhabitants living nearby.

Geographic Information Systems (GISs) are suitable tools for analysing and visualising spatial information. GISs have been used in energy applications from resource assessment to infrastructure planning. GISs can be used to develop spatial decision support systems which are designed to help decision makers solve spatially related problems by integrating data management and capabilities such as analytical and spatial modelling, spatial display and reporting [l4]. GISs handle data in digital models; one of most useful is the raster data model. The raster data model divides the studied geographic area into a regular grid of GIS cells where each cell contains the value of a variable of interest and a geographical position.

GISs have been used in the VIA of new wind farms. In [12] a GIS was used to generate 3D maps of a proposed area for a new wind farm. Rodrigues et al. [15] take into account four parameters for the VIA of a new wind farm: orography, land-cover height, the facility height and width, and the observer height. The population in the vicinity and the users of roads and railways are also considered, and the distance to the facility is included as a divisor of a visual impact index. The authors calculate the visual impact indexes for six energy production scenarios. The results show the relationship between the number of wind turbines and the visual impact index values. Manchado et al. [16] use a GIS to determination potentially suitable areas for the installation of new wind farms, taking into account the visibility assessment. A whole geographic area is analyzed in order to identify the zones where the new wind farm has lower visibility from population nuclei.

Wind farms are the most prolific renewable energy based power plants with a greater geographical diffusion, although large-scale PV power plants, with a capacity comparable to that of medium sized wind farms or even greater, are being developed all over the world [17]. The size of large PV plants, their regular geometry, and the highly reflective surface of the panels used, make these plants visible for long distances and they may contrast with surrounding natural or rural settings [18]. In the visual impact assessment of PV plants, the distance between the facility and the observer also has a relevant importance. This parameter is considered as the most important among others that include the effect of the scale, topography, vegetation and weather [19].

A similar methodology to that which is applied to wind farms in [13] was applied to solar power plants by the same authors [20]; in this case the continuity factor was changed to a concurrence factor, related to the concentration of solar panels. The risk of glare from PV plants is focused on [21], with a study of the visual impact produced by a PV plant with 3085 modules sited in Italy. The authors conclude that although glare can increase the visual impact, this only takes place for very short time periods and so can be neglected.

So, even though a major effort has been undertaken in order to evaluate the VIA of new power plants based on renewable energies, it has mainly been carried out for wind farms, and even in those cases with an *a posteriori* analysis: once the power plant has been designed, the VIA is calculated. Only a few works [15, 16] describe the VIA, for new facilities, over a whole area in order to select the locations with lower visual impact.

The visual impact that a new power plant can cause is directly related to its observability. When the plant is not visible from the places frequented by people, its visual impact will be negligible. The visual impact of the plant increases when it is visible from more places and for more people. Even with a fixed number of people for whom the plant is visible, its visual impact is raised with an increase in the possible hours of observation.

This paper presents a new methodology, based on GIS, for ranking the places in a zone according to the observability of a new PV power plant. We define a new variable called the Potential Observation Hours (POH), which represents the aggregated value of the maximum number of hours in a mean day in which an object may be viewed by each possible observer. This is related to the inhabitants in the zone, the size of the object, the possible observers from paths and roads, and their distance to the observed object. With the evaluation of the POH variable for all the cells (in a GIS) representing a geographical zone, a map can be obtained. This map helps to visually identify the places in the zone with the highest or lowest observability. The proposed methodology can be easily adapted to other kinds of power plants (wind, thermo-solar, etc.), only changing the height, cell size and extension occupied by the power plant. This methodology can be useful to local authorities who have to authorize the installation of the new power plant in the territory under their competence, or investors who are trying to find the best locations from the point of view of visual impact or visibility.

The paper is structured as follows: the second section presents the methodology used for the evaluation of the POH for each cell (representing a geographical area) in a GIS and the development of maps for the zone under study; the third section shows two case studies with the application of the proposed methodology for the selection of locations for the installation of two kinds of PV plants (0.6 MWp two-axis tracking system PV plant, and a 1 MWp grid-connected fixed panel PV plant, both located in rural zones in La Rioja, Spain); finally, the conclusions are presented in the last section.

2. Description of the proposed methodology

The main goal of the proposed methodology is the achievement of a set of GIS maps which help to visually identify the places in a zone with the lowest observability. These maps are built with the POH variable which takes into account all the possible observers (in motion or on-site). This variable depends mainly on the characteristics of the terrain in the studied area (orography, represented in the GIS by the Digital Terrain Model, DTM). It also depends on existing communities in the area (observation points and on-site observers), existing roads that connect these communities (moving observers), and PV plant characteristics (height of panels, extension of land occupied, etc.).

The POH values are stored in raster format in a GIS. The raster format keeps the geographical information in cells that represent a small square area in the geographical zone under study. In the GIS, a numerical value is associated to each cell of the raster format. In order to store values for different variables or results, a set of raster files can be used, where the cells present the same geographical reference in all the files.

For a single observation on-site point (village, hamlet, farm, viewpoints, etc.) and for a single road segment, we define the POH as a numerical value that depends on the number of potential affected observers and on the distance between them and the observed object. The distance plays a key role because human visual acuity diminishes with distance [22]. The POH also depends on the orography of the terrain between the observation point and the observed object.

Some published works relating to GIS applications have proposed methods to take into account the distance in the human visual acuity formulation. So, Fisher proposed the fuzzy viewshed method in 1994 [23]. This method aims to take into account the fact that an object can be seen to a different degree of clarity under different circumstances. The author applies fuzzy membership functions, the values of which decay with the increase in distance from the observer to analysed location.

The size of the observed object in the analysed location and the distance from the observer are taken into account jointly by Ogburn [24]: the author applies the fuzzy viewshed approach modified to account for target size. In that work, the author establishes that there are no set formulae that directly factor in the limits of human visual acuity, atmospheric extinction (degradation of visibility over distance), and the physical properties of objects and their surroundings. So, he proposes the use of fuzzy membership values obtained with the application of a distance decay function which declines with distance in relation to the size of the observed object. The parameters of the decay function are calculated taking into account that the distance at which an object reaches the standard limit of recognition acuity, i.e., the point at which it subtends a visual arc of 1′. This limit of recognition acuity is also known as 20/20 vision. The distance decay function is shown in (1), where x represents the position of the observed object, d is the distance between the position of observer and x, b_1 is the limit (distance from the observer) of the foreground zone of high clarity, and the sum of b_1 and b_2 corresponds to the distance where an object of the width of the observed object subtends a visual arc of

1′. Parameters b_1 and b_2 depend on the size of the observed object. We have used for b_1 the distance corresponding to the limit of short-distance view defined by Higuchi [25], that is the distance at which the observed object subtends a visual arc of 1º. The fuzzy membership values obtained with (1) range 0 to 1, giving a value of 0.33 to the 1′ visual threshold.

$$\begin{cases} \mu(x) = 1 \quad \text{for } d \le b_1 \\ \mu(x) = \dfrac{1}{1 + 2\left(\dfrac{d - b_1}{b_2}\right)^2} \quad \text{for } d > b_1 \end{cases} \tag{1}$$

This distance decay function can be easily adopted for a GIS environment. The position of the observed object can be represented by a cell in a GIS raster format, and d corresponds to the distance between the central position of the area represented by that cell and the position of the observer. For a single observer, the value obtained with (1) represents the fuzzy membership value for the object placed in position (cell) x. Fig. 1 plots the distance decay function corresponding to an object with a size of 10 m. The values of parameters b_1 and b_2 are 570 m and 33800 m, respectively.

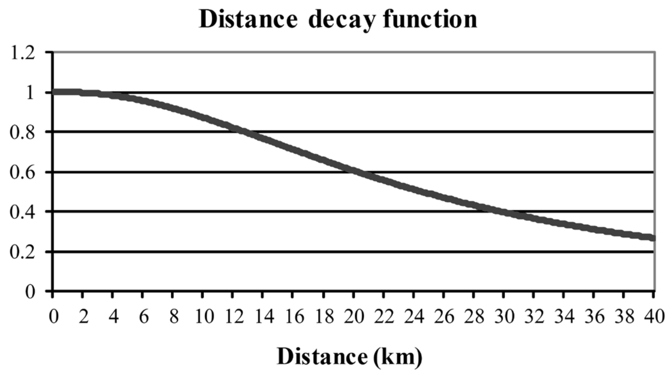

Fig. 1. Distance decay function for an object with a 10 m size.

We propose the use of the distance decay function in order to calculate the POH, because it takes the size of the observed object into account. Since the height for a PV plant is usually less than its width, we take only the height into account as a measurement of its size. The number of possible observers and the orography between these observers and the object also influence in that calculation, as it is described in the next section. The starting point is the DTM corresponding to the geographic zone where the new PV plant would be built. The geographic zone is represented by a set of regular cells in the GIS. The size of the cells is chosen according to the real size of the PV plant (it must occupy the area represented by only one cell).

2.1. On-site observers

Initially, the data corresponding to the on-site observation points are stored in an on-site observer table. This table contains the geographical position of each observation point, the observer height above the ground and the number of potential observers. These potential observers can correspond to inhabitants in communities or single observation on-site points, or to average daily visitor in viewpoints, monuments, natural parks, etc. The calculation process of the POH corresponding to a facility placed in the area represented by the cell i in a GIS and to an observation point j, $POH_{i,j}$, is shown in Fig. 2. The stages of the process are as follows:

1. The data corresponding to the height above the ground and the land area of the PV plant are stored in the GIS in the cell i.
2. The data corresponding to observer height above the ground and number of potential observers from the observation point j are read from the on-site observers table.

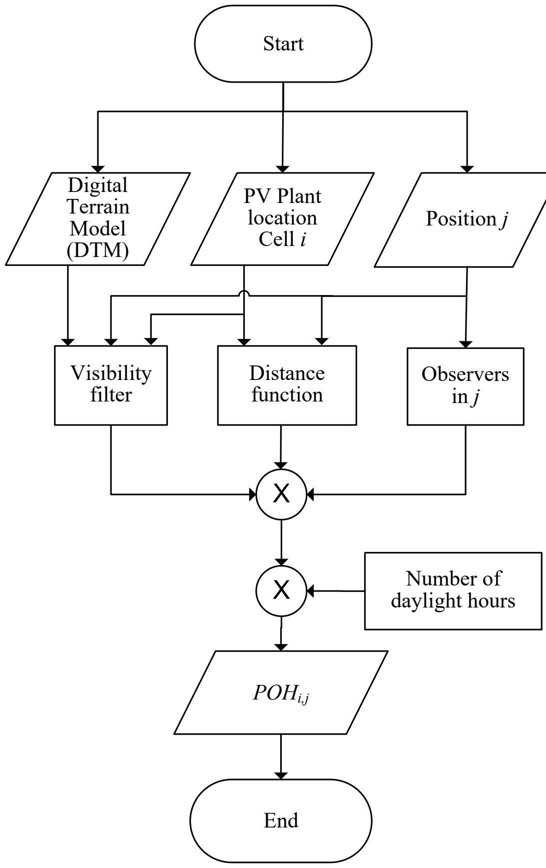

Fig. 2. POH calculation flow-chart for a PV plant in cell i, and observers in position j.

3. Application of a "visibility filter":
   For on-site observers, this filter corresponds to a function which returns a value 0 if the PV plant in a position or cell i (with the characteristics stored initially) is not visible from position j (with the height read in stage 2). This filter returns a value 1 when the PV plant in cell i is visible from the position j. The visibility filter value is stored in cell i.
4. The GIS calculates the Euclidean distance between the centre of the area represented by cell i (PV plant) and the position j (observers).

5. The GIS calculates the value for the distance decay function (value returned by the function according to the distance between the PV plant and the observers).
6. The GIS multiplies the value obtained with the visibility filter, the value for the distance decay function, the number of possible observers in position j and the number of daylight hours of a mean day (12 hours). The result corresponds to the POH generated by the PV plant in the area represented by the cell i, taking into account only one community or a single observation on-site point j, $POH_{i,j}$.

Steps 2 to 6 are repeated for all the on-site observation points (a total of M observation points, each one with a different position, height and number of possible observers) in the zone under study and surroundings. The values obtained, $POH_{i,j}$ for each observation point, are aggregated to obtain the On-Site Global Potential Observation Hours value, $OSGPOH_i$ (2), that is, the aggregated value of the maximum number of observation hours in a mean day for all the possible on-site observers. With this action, we obtain a numeric value that is stored in the cell corresponding to the position i.

$$OSGPOH_i = \sum_{j=1}^{M} POH_{i,j} \tag{2}$$

2.2. On-road observers

The POH calculation process is slightly different to that one for on-site observers. In this case, the possible observers are travelling along a road. In order to evaluate the number of possible on-road observers, the average daily traffic (ADT, that is, the average number of vehicles per day) is used; this value can be obtained from local authorities. Each road in the studied zone is divided into segments. A segment is the stretch of road whose nodes have the same ADT value. Initially the data corresponding to on-road observers are stored in a table (on-road observers table). This table includes, for each road segment, the number of possible observers (its ADT value multiplied by the average number of occupants per vehicle), its length, and the average speed of the vehicles in that segment. We suppose the same height over the road for all the on-road observers.

In the process of calculation, each road segment is divided into evenly separated nodes. Each node corresponds to an observation point in the GIS. The process, for the road segment k, is as follows:

1. The data corresponding to the height above the ground and the land area of the PV plant are stored in the GIS in the cell i.
2. Data corresponding to the road segment k are read from the table.
3. Application of the “visibility filter”:
   For on-road observers, this filter corresponds to a function which returns the number of nodes from which the area represented by cell i is visible.
4. The GIS calculates the Euclidean distance between the centre of the area represented by cell i (PV plant) and the road segment k.

5. The GIS calculates the value corresponding to the distance decay function (value returned by the function according to the distance between the centre of the area represented by the cell *i* and the segment road *k*).
6. The GIS multiplies the value obtained with the visibility filter, the value corresponding to the distance decay function, the number of potential observers, and the distance from node to node of the road segment *k*. This product is divided by the average speed of the vehicles in that road segment. The result corresponds to the POH caused by the PV plant in the cell *i*, taking into account only the road segment *k*, $POH_{i,k}$.

The flow-chart for this process is similar to the one represented in Fig. 2, changing "Position *j*" for "Road segment *k*", "Observers in *j*" for "Observers in road segment *k*", and "Number of daylight hours" for "Distance from node to node node divided by the average speed of the vehicles in that road segment".

This process is repeated for all the possible on-road observers (a total of *K* road segments corresponding to all the roads) in the zone under study and surroundings. Moreover, the values obtained $POH_{i,k}$ for each road segment are aggregated by (3) to obtain the On-Road Global Potential Observation Hours value, $ORGPOH_i$, that is, the aggregated value of the maximum number of observation hours in a mean day for all the possible on-road observers. The numeric value obtained is stored in the cell corresponding to the position *i*.

$$ORGPOH_i = \sum_{k=1}^{K} POH_{i,k} \tag{3}$$

The suggested process can be easily modified in order to consider all kind of mobile observers, from pedestrians on a path to passengers in a train. All that is needed is to include a new column with the height of the observers above the road, path or railroad in the on-road observers table.

2.3. Normalized Index Maps

A set of maps related to the POH of the new PV plant can be obtained if the previously presented process is applied to all of the cells that correspond to the zone under study (all the possible positions *i*). The maps are built representing each cell in the map with a colour denoting the value, in that cell, of the variable represented in the map. For example, using the *OSGPOH* variable and a monochromatic colour scale, we can build the *OSGPOH* map, where the areas with lower or higher values (lighter or darker colours) are easily identifiable If the value of the variable of interest in each cell is normalized with respect to the highest value of that variable for all the cells in the zone under study, we can obtain a normalized index map, where all the cells present values between 0 and 1. So, we can obtain the normalized *OSGPOH* and *ORGPOH* values using (4), where max(*OSGPOH*) and max(*ORGPOH*) correspond to the maximum values, for all the cells, of both variables.

$$\begin{cases} nOSGPOH_i = \dfrac{OSGPOH_i}{\max(OSGPOH)} \\ nORGPOH_i = \dfrac{ORGPOH_i}{\max(ORGPOH)} \end{cases} \quad (4)$$

A normalized map represents a ranking of the areas where it is possible to build the new PV plant. Cells with the lowest values correspond to the areas with the lowest POH in the zone, while cells with value 1 correspond to the areas with the greatest one. Cells with value 0 correspond to areas with a null visual impact, because they are not observable either by on-site observers or by on-road observers.

In order to include on-site and on-road observers in a single map, two different strategies can be chosen:

A) The normalized POH variables, that is, the variables *nOSGPOH* and *nORGPOH*, are combined by (5) to obtain the Global Potential Observation Hours Index, *GPOHI*. Both values are aggregated in each cell with normalized weights ($w_s+w_r = 1$) to assign the importance and quality of every type of observer.

$$GPOHI_i = w_s \cdot nOSGPOH_i + w_r \cdot nORGPOH_i \quad (5)$$

The variable obtained with this operation, *GPOHI,* can be represented in a map in which each cell (position *i*) presents a value between 0 and 1. This value is a relative index.
Note that, with this strategy, the weights are assigned to the type of observer, on-site or on-road. This strategy can be useful in zones with a very different number of possible observers and there are reasons to increase the importance of one kind or another: touristic zones, road accesses to natural parks, etc. In order to avoid the penalization of possible on-site observers, this strategy must be chosen when the possible on-road observers aren't mainly inhabitants in the zone under study: on-site observers are visually affected every day, meanwhile on-road observers may be affected only occasionally.

B) The POH variables, that is, the variables *OSGPOH* and *ORGPOH*, are combined by (6) to obtain the normalized Global Potential Observation Hours, *nGPOH*. The values are aggregated in each cell with normalized weights ($w_s+w_r = 1$) and normalized with respect to the highest value for all the cells in the zone under study (in the denominator).

$$nGPOH_i = \frac{w_s OSGPOH_i + w_r ORGPOH_i}{\max(w_s OSGPOH + w_r ORGPOH)} \quad (6)$$

The variable obtained with this operation, *nGPOH*, can be also represented in a map in which each cell (position *i*) presents a value between 0 and 1. In this case the cells with value 1 correspond to those areas with the highest POH in the studied zone.
This strategy can be used in zones where there is an interest in aggregating on-site and on-road observers in order to obtain a joint ranking. The values of POH, on-site and on-road, are aggregated, although the use of weighting factors can assign more importance to one or another of the type of observer. This strategy must be chosen when the on-site observers and the on-road observers are almost the same: the roads are used mainly by the inhabitants in the zone.

3. Case studies

We present two case studies for different zones. In the first case study we consider the installation of a new PV plant in a zone where most of the users of the roads are not inhabitants of the zone. In the second case study we consider the installation of a new PV plant in a zone where the roads are mainly used by the inhabitants of their own zone. In both cases the PV plant will be installed inside a municipal territory. The selected zones correspond to the municipal territories of Aldeanueva de Ebro (case study 1), and of Arnedo (case study 2). Both zones are situated in La Rioja, Spain, a region famous for its wines and with social interest in maintaining the landscape with vineyards as a tourist claim. So, for both case studies, the methodology is used to identify the places with the lowest observability. Fig. 3 shows the two selected zones, which are separated by less than 10 km.

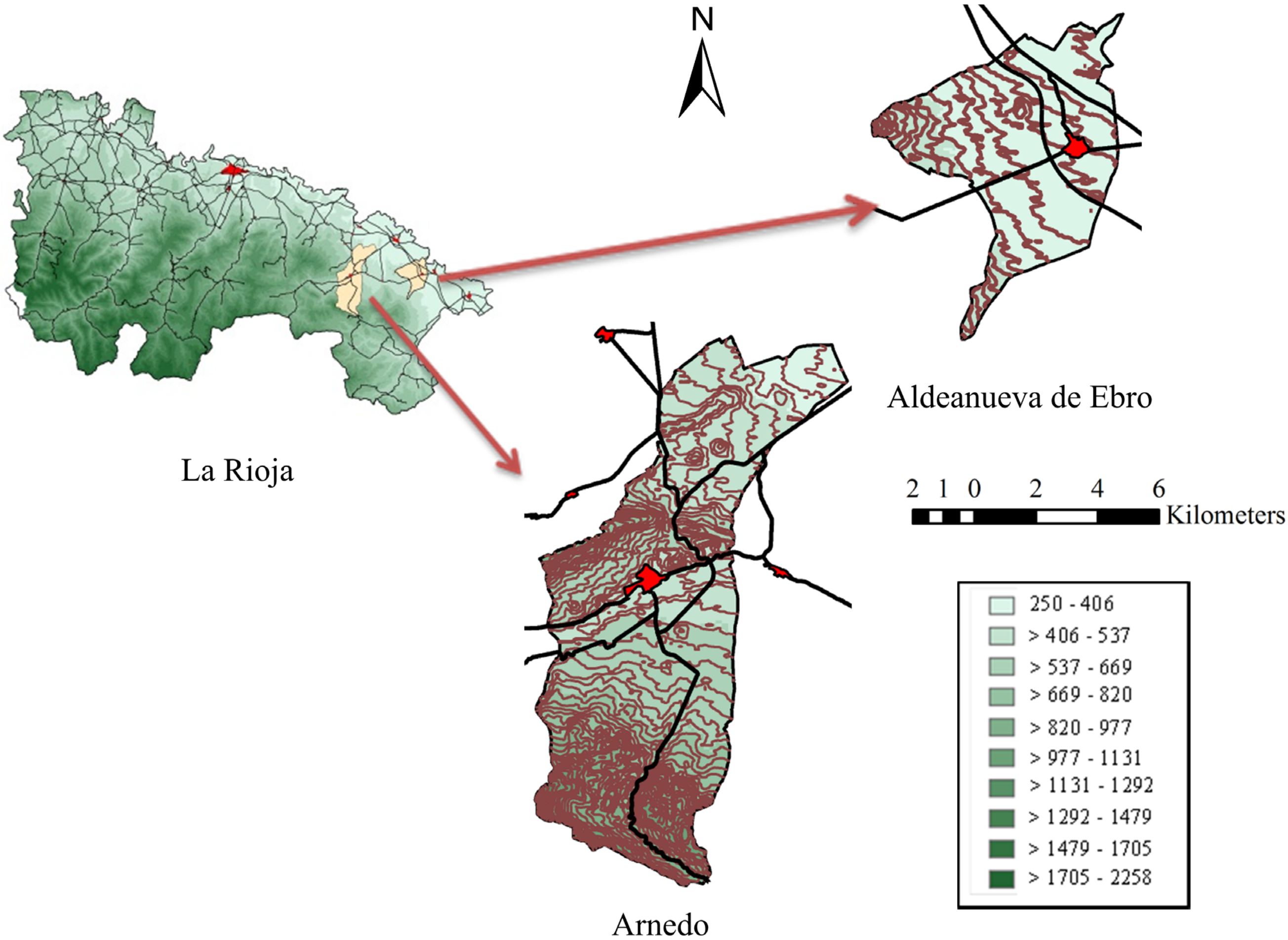

Fig. 3. DTM of La Rioja where the zones under study and the main human communities and roads are represented. The values in the legend correspond to height above sea level in metres.

In order to apply the proposed methodology, all the human communities in the zones under study and in the surrounding areas were taken into account, with a total (for both cases) of 22 communities including towns, villages and hamlets. The number of inhabitants in the communities considered ranges from 24500 (the town of Calahorra) to 8 (a little hamlet).

The traffic measurement stations in the zones chosen for both case studies are shown in Fig. 4. Traffic measurements have been taken from government sources [26]. In that figure, the denomination of the measurement station, the ADT value (IMD in Spanish), and the percentage of heavy vehicles (%P) are represented in boxes, and the measurement stations are marked with stars. In the case studies we considered all the stretches between two bifurcations as road segments, although shorter segments could be chosen. Each road segment was divided in nodes (one per meter of length). The total number of road segments for each case study was 53.

The case studies were carried out to identify the best areas, following visual criteria, for the installation of two different PV plants with a common characteristic: their construction needs the same surface area. Although both plants need the same surface area, the rated electrical power of the PV plants is different. The two PV plants are the following: a PV plant with solar trackers, with seven meters average height, and an installed nameplate capacity of 0.6 MWp (in DC and under Standard Test Conditions) in the case study 1, and a PV plant with fixed ground-mounted panels, with two meters average height, and a capacity of 1 MWp in the case study 2. The approximate surface area for each of these facilities is 10000 m2, having taken into account the latitude and the average solar irradiation in those zones. Therefore, we selected a GIS cell size of 100x100 m. So, each cell, representing an area of 10000 m^2 in the studied zones, corresponds to a potential site for the construction of the selected PV plant.

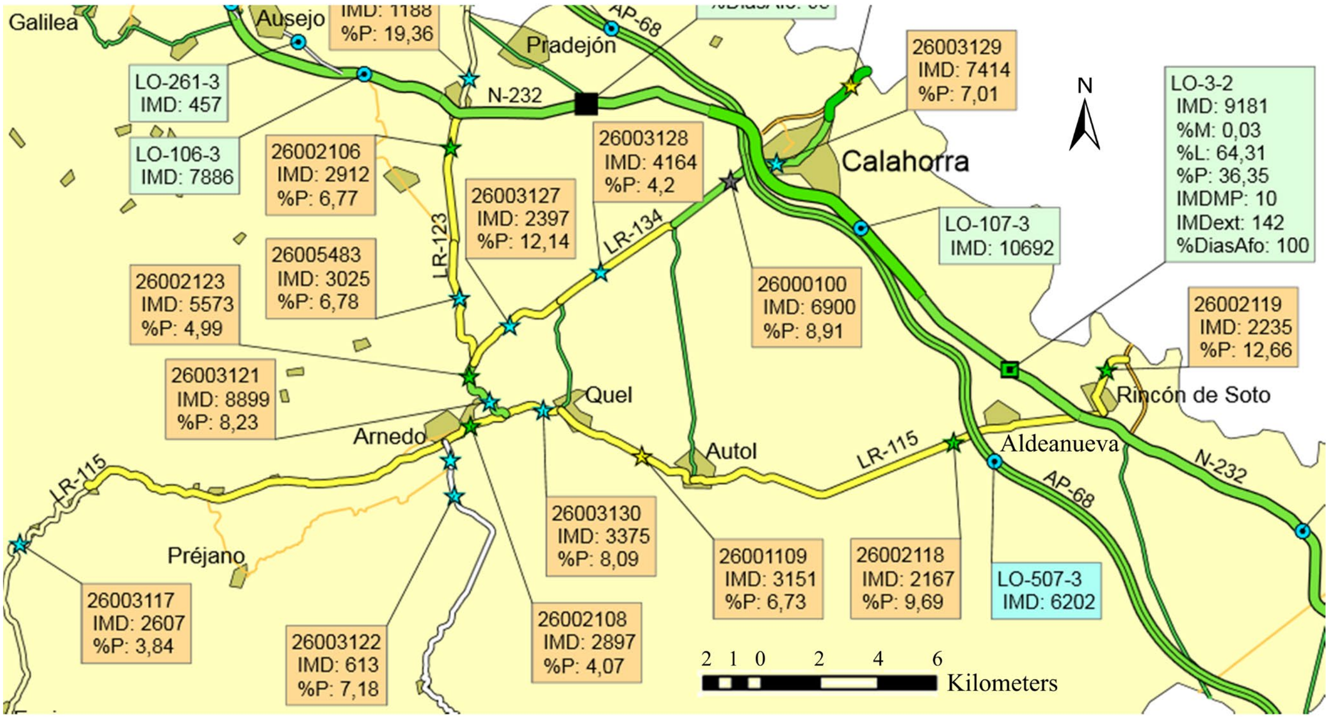

Fig. 4. Data of traffic on the roads corresponding to the studied area.

Case study 1

In this first case study the new facility corresponds to a two-axes solar tracker PV plant with a capacity of 0.6 MWp. The new PV plant will be constructed in the municipal territory of Aldeanueva de Ebro, in La Rioja (Spain). The considered height over the ground is 7 meters and the surface area needed is 10000 m^2. The municipal territory of Aldeanueva de Ebro, with approximately 39 km^2, has an irregular shape (Fig. 3) and was selected as the zone under study. The main community in that zone is the village of Aldeanueva (2800 inhabitants). Two main roads cross the municipal territory, a highway and a major road. The users of these roads aren't usually inhabitants of the zone or of the surroundings. So, in this case study we used the proposed methodology with strategy A.

Fig. 5a shows the *OSGPOH* map and Fig. 5b shows the *ORGPOH* map. The limits of the municipal territory of Aldeanueva are represented in black, the area occupied by the urban centre is represented in yellow, and the roads are represented by lines. Areas with low-height level are situated on the top right and correspond to the flood plain of the river Ebro. The urban centre is slightly above the height of the flood plain; though lower than most of the other areas in the municipal territory.

In the maps shown in Fig. 5, the green colour represents the cells with a null value of POH. In general, areas surrounding the urban centre have high values of *OSGPOH*, except those areas that cannot be seen from there (areas situated to the west or south of the urban centre). The *ORGPOH* map shows that the highest values correspond to areas that can be seen from most of the road segments and not necessarily to the areas adjacent to the highway or local roads.

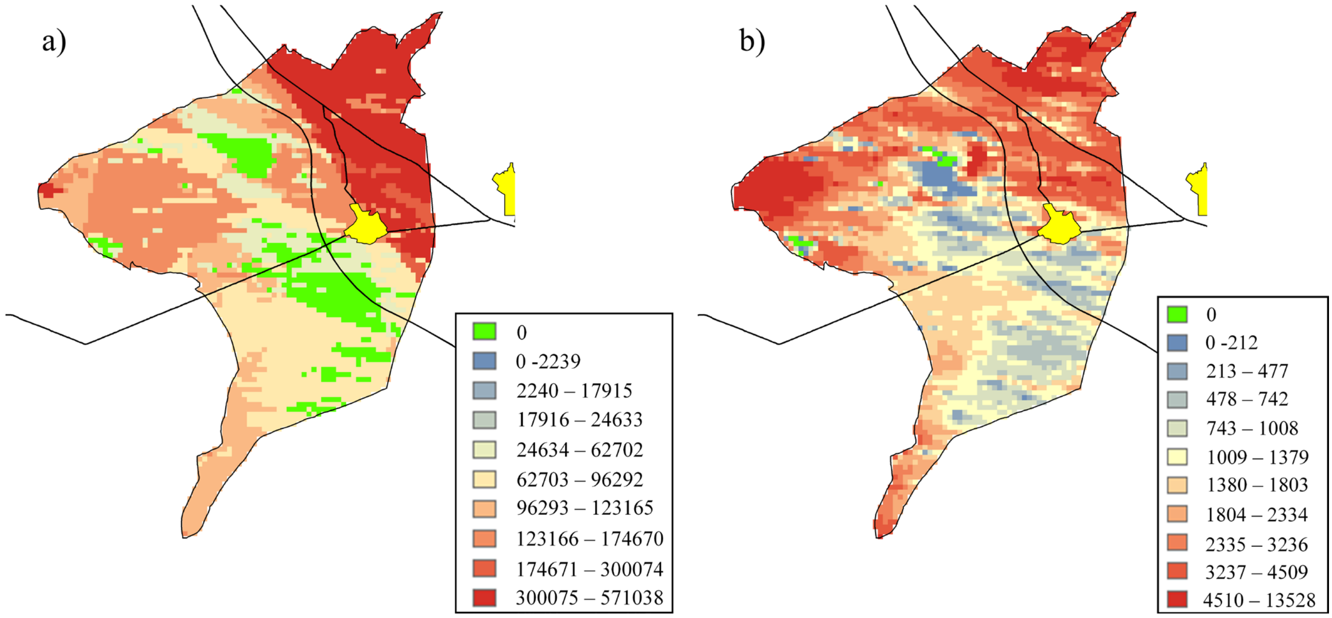

Fig. 5. a) OSGPOH map. b) ORGPOH map.

Fig. 6 shows the *GPOHI* map, obtained with normalized weights $w_s = 0.8$ and $w_r = 0.2$. Note that the areas with null values for the *OSGPOH* and *ORGPOH* variables, present a null value again. There are 18 cells with a null value of the *GPOHI*, which corresponds to areas with 0.18 km^2, where the visual impact of the new PV plant with the above-mentioned characteristics is negligible (the PV plant will not be seen for any observer, on-site or on-road). Fig. 7 presents the histogram corresponding to the *GPOHI* variable which shows that 767 cells present values lower than 0.0117 (12.4% of the maximum value which is 0.944).

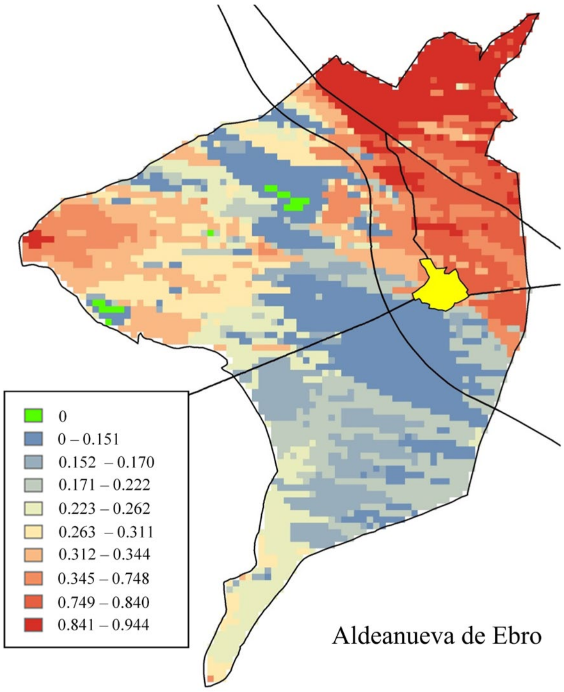

Fig. 6. GPOHI map obtained with weights w_s=0.8 and w_r=0.2.

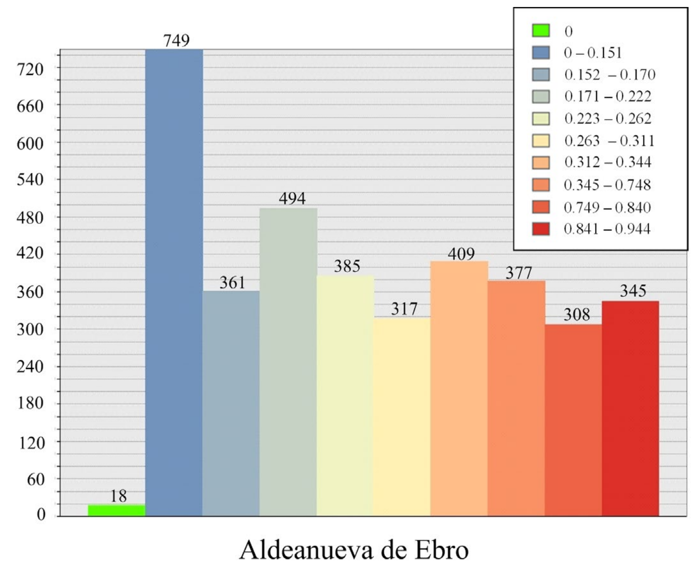

Fig. 7. Histogram corresponding to the GPOHI variable.

Case study 2

In this second case study the new facility corresponds to a fixed, ground-mounted panel PV plant with a capacity of 1 MWp. The PV plant will be constructed in the municipal territory of Arnedo, in La Rioja (Spain). The height of the panels over the ground is two meters and the surface area needed is 10000 m^2. The municipal territory of Arnedo, with approximately 86 km^2, has the shape showed in Fig. 3, and was selected as the zone under study. The main community is the town of Arnedo (14500 inhabitants), situated near the centre of the zone. The roads in the zone connect the town of Arnedo with the nearby communities, and they are mainly used by the inhabitants in the zone. The two main roads in the surroundings (the same ones as in the first case study) hardly affect the POH results in this zone because the municipal territory is in a valley that is not crossed by those roads.

The methodology described in section 2, with strategy B, was applied in order to obtain the POH in all the cells in the area under study. Fig. 8a shows the *OSGPOH* map and Fig. 8b shows the *ORGPOH* map. The limits of the municipal territory of Arnedo are represented in black, the urban centre is represented in yellow, and the roads are represented by lines. In both maps, the green colour represents the cells with a null value of POH. The north part of the municipal territory shows low values of *OSGPOH*. Areas surrounding the urban centre in east direction have high values of *OSGPOH*, except those areas that cannot be seen from there. This is because it is located along a river, in a terrain depression, and there are nearby areas that cannot be seen from the urban centre. The highest values of ORGPOH correspond to areas that can be seen from most of the road segments (note that the road segments considered are not only those inside the territory, but all the ones in the surroundings). There are some areas with null values for the *OSGPOH* and the *ORGPOH*, even near the urban centre.

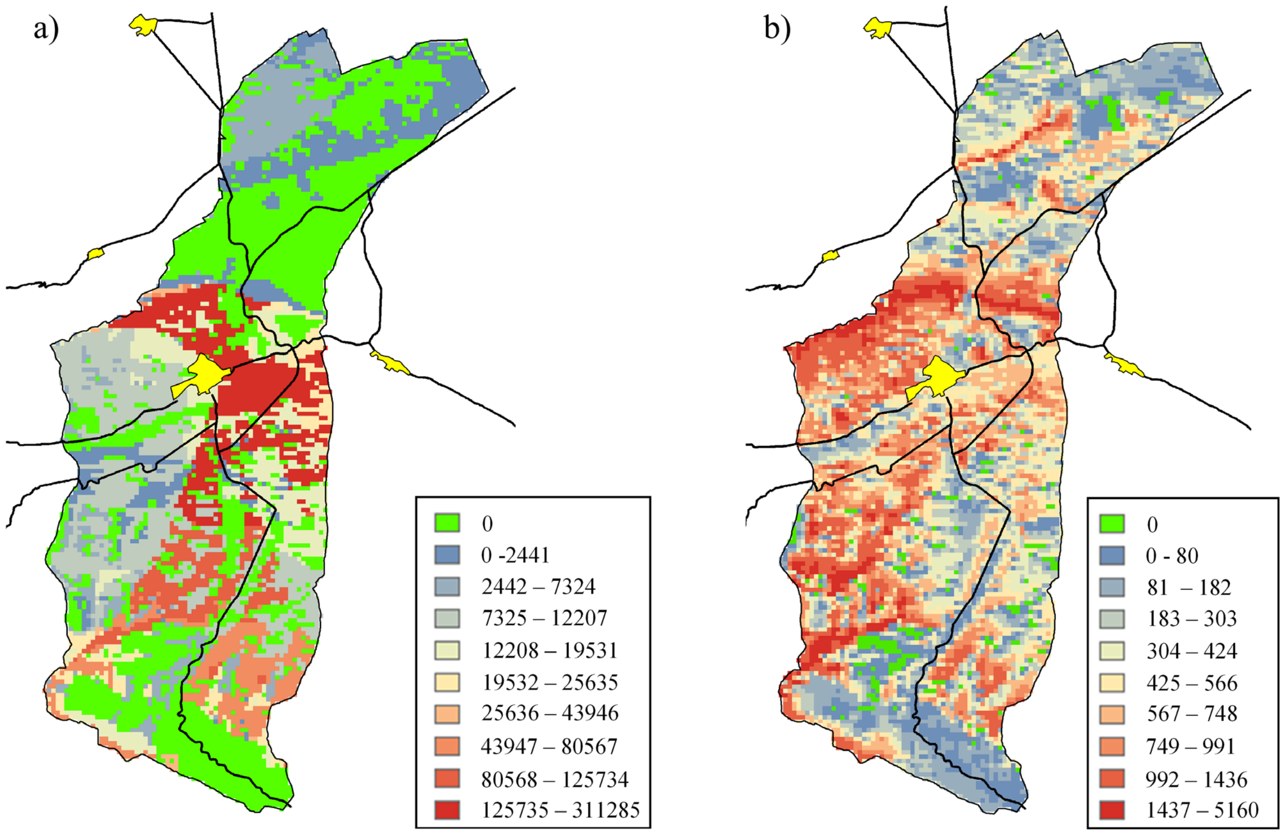

Fig 8. a) On-Site Global Potential Observation Hours Map. b) On-Road Global Potential Observation Hours Map.

Fig. 9 shows the *nGPOH* map, obtained with normalized weights w_s = 0.5 and w_r = 0.5. We have assigned the same value to both weighting factors because the on-road observers are mainly local inhabitants. In the map there are 245 cells, which represent a total surface area of 2.45 km^2, with a null *nGPOH* value. These areas are the best ones to install the new PV plant, because they have a null visual impact (they are not visible from the communities in the zone under study nor from the surroundings, nor from the roads). Areas surrounding the urban centre to the north and to the east present the highest values of *nGPOH* (cells with the red colour), while the areas with the lowest values are located mainly to the north of the municipal territory. Fig. 10 shows the histogram of the *nGPOH* variable, where near 44% of the cells present values lower than 0.0117, while only 6% of the cells present values over 0.8.

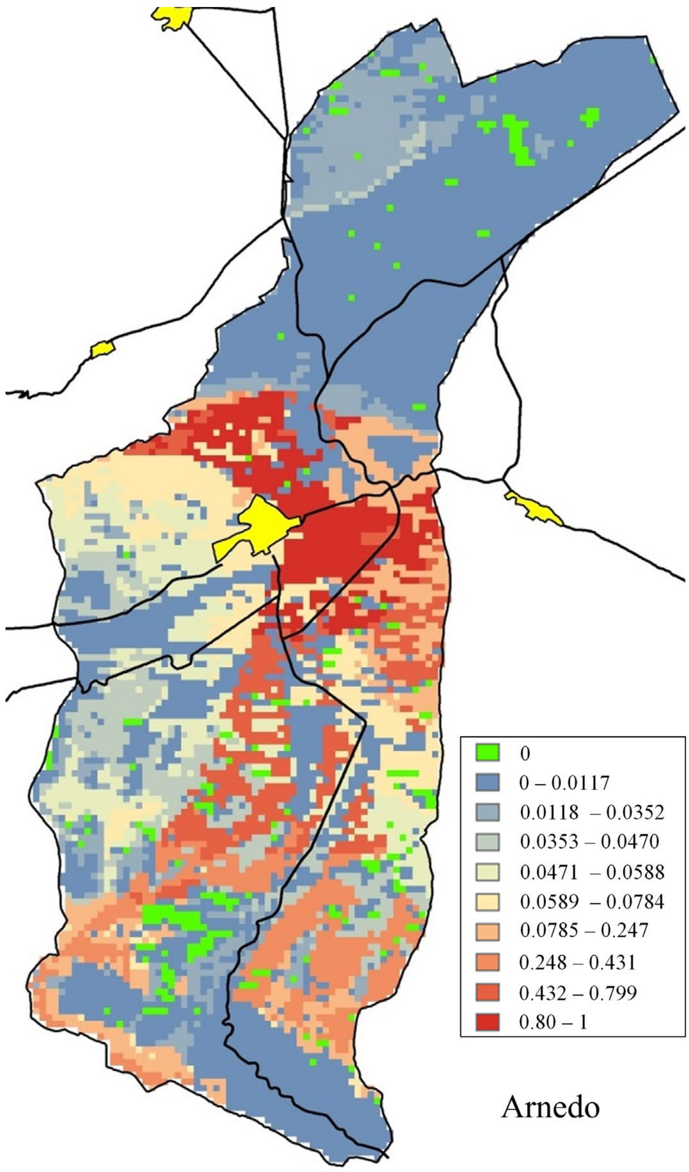

Fig. 9. nGPOH map with a 0.5 value for both weighting factors.

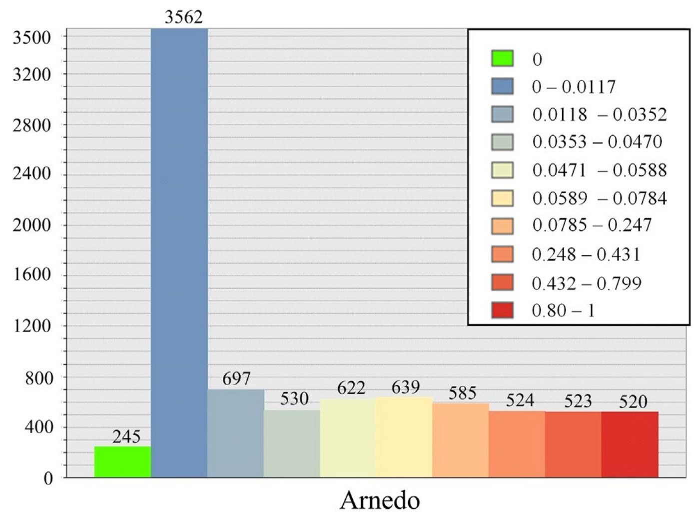

Fig. 10. nGPOH histogram.

In both case studies, the results obtained offer, in a visually friendly format, valuable information to the municipal authorities that have to approve the installation of the new PV plant or to promoters that are supporting its construction. All the areas in the municipal territory are classified according the POH value, allowing the selection of those areas with the lower values.

4. Conclusions

A new methodology for ranking the places in a zone according to the observability of a new medium size PV plant has been described. It is based on GIS, what allows the presentation of visual maps. The possible observers considered include both inhabitants in the studied zone and in the surroundings, as well as travellers crossing it by road. The visual effect on the possible observers is evaluated by a new variable called the Potential Observation Hours (POH). This variable depends on the number of possible observers, on-site and on-road, and on the distance to the PV plant, with a function which depends on its size. The POH value corresponds to the aggregated value of the maximum observation hours for all the possible observers in a mean day. This variable allows the classification of the areas in the zone under study from the lowest to the highest observability corresponding to a new PV plant built on it.

The POH variable can be represented graphically, for all the areas in a zone, as a set of maps. These maps help to identify the areas with the maximum or minimum observability in the zone. Since the observability is related to the visual impact caused by a new PV plant, the proposed methodology can contribute to speeding up its construction as a result of the selection of the locations with lower visual impact or with higher visibility. Any PV plant promoter can easily identify, on the corresponding map, the optimal places for the new PV plant, which means that the time needed to obtain the permissions from the local authorities may be shorter.

The proposed methodology can be adapted to any kind of power plant, if its characteristics (surface size and height), the DTM of the zone, as well as the distribution of the inhabitants, workers or visitors at each possible observation point or road links are known.

Acknowledgments

The authors would like to thank the ‘‘Ministerio de Economia y Competitividad’’ of the Spanish Goverment for supporting this research under the project ENE2013-48517-C2-2-R and the ERDF funds of the European Union.

References

[1] Haas R, Panzer C, Resch G, Ragwitz M, Reece G, Held A. A historical review of promotion strategies for electricity from renewable energy sources in EU countries. Renewable and Sustainable Energy Reviews 2011; 15 (2): 1003-1034.

[2] International Energy Agency, Technology Roadmap: Solar photovoltaic energy, IEA 2010. Available on-line: http://www.iea.org/publications/freepublications/publication/pv_roadmap.pdf

[3] Goetzberger A, Hoffmann VU. Photovoltaic Solar Energy Generation. Springer. Berlin, 2005.

[4] Arán Carrión J, Espín Estrella A, Aznar Dols F, Zamorano Toro M, Rodríguez M, Ramos Ridao A. Environmental decision-support systems for evaluating the carrying capacity of land areas: Optimal site selection for grid-connected photovoltaic power plants. Renewable and Sustainable Energy Reviews 2008; 12: 2358–2380.

[5] Haurant P, Oberti P, Muselli M. Multicriteria selection aiding related to photovoltaic plants on farming fields on Corsica island: A real case study using the ELECTRE outranking framework. Energy Policy 2011; 39 (2): 676-688.

[6] Wüstenhagen R, Wolsink M, Bürer M J. Social acceptance of renewable energy innovation: An introduction to the concept. Energy Policy 2007; 35 (5): 2683-2691.

[7] Heras-Saizarbitoria I, Cilleruelo E, Zamanillo I. Public acceptance of renewables and the media: An analysis of the Spanish PV solar experience. Renewable and Sustainable Energy Reviews 2011; 15 (9): 4685-4696.

[8] Ribeiro F, Ferreira P, Araújo M. The inclusion of social aspects in power planning. Renewable and Sustainable Energy Reviews 2011; 15: 4361– 4369.

[9] Gamboa G, Munda G. The problem of windfarm location: A social multi-criteria evaluation framework. Energy Policy 2007; 35 (3): 1564-1583.

[10] Hurtado J P, Fernández J, Parrondo J L, Blanco E. Spanish method of visual impact evaluation in wind farms, Renewable and Sustainable Energy Reviews 2004; 8 (5): 483-491.

[11] Tsoutsos T, Tsouchlaraki A, Tsiropoulos M, Serpetsidaki M, Visual impact evaluation of a wind park in a Greek island, Applied Energy 2009; 86 (4): 546-553.

[12] Molina-Ruiz J, Martínez-Sánchez M J, Pérez-Sirvent C, Tudela-Serrano M L, García Lorenzo M L. Developing and applying a GIS-assisted approach to evaluate visual impact in wind farms. Renewable Energy 2011; 36: 1125-1132.

[13] Torres Sibille A C, Cloquell-Ballester V A, Cloquell-Ballester V A, Darton R. Development and validation of a multicriteria indicator for the assessment of objective aesthetic impact of wind farms. Renewable and Sustainable Energy Reviews 2009; 13: 40–66.

[l4] R. Sugumaran, J. Degroote, Spatial Decision Support Systems. Principles and Practices. CRC Press, Boca Raton, Florida, 2011.

[15] Rodrigues M, Montañés C, Fueyo N. A method for the assessment of the visual impact caused by the large-scale deployment of renewable-energy facilities. Environmental Impact Assessment Review 2010; 30 (4): 240-246.

[16] Manchado C, Otero C, Gómez-Jáuregui V, Arias R, Bruschi V, Cendrero A. Visibility analysis and visibility software for the optimisation of wind farm design. Renewable Energy 2013; 60: 388–401.

[17] World's Largest Photovoltaic Power Plants. PV resources 2009 [Online]. Available: http://www.pvresources.com/en/top50pv.php

[18] Sullivan R G, Kirchler L B, McCoy C, McCarty J, Beckman K, Richmond P. Visual Impacts of Utility-scale Solar Energy Facilities on Southwestern Desert Landscapes. Argonne National Laboratory Report, Available online: http://visualimpact.anl.gov/solarvis/docs/Solar_Visual_Impacts.pdf (accessed on 4th October 2013).

[19] SRK Consulting, Draft Visual Impact Assessment for the proposed SATO holdings Photovoltaic project, near Aggeneys, Northern Cape, Sato Energy Holdings Report, No. 435209_VIA, 2012.

[20] Torres Sibille A C, Cloquell-Ballester V A, Cloquell-Ballester V A , Darton R. Aesthetic impact assessment of solar power plants: An objective and a subjective approach. Renewable and Sustainable Reviews 2009; 13: 986-999.

[21] Chiabrando R, Fabrizio E, Garnero G. The territorial and landscape impacts of photovoltaic systems: Definition of impacts and assessment of the glare risk. Renewable and Sustainable Energy Reviews 2009; 13 (9): 2441-2451.

[22] Schiffman H R. Sensation and Perception: An Integrated Approach. 5th ed. New York: Wiley; 2001.

[23] Fisher P F. Probable and fuzzy models of the viewshed operation. In: M.F. Warboys (Ed.), Innovations in GIS 1, Taylor & Francis, London, 1994, pp. 161-175.

[24] Ogburn D E. Assessing the level of visibility of cultural objects in past landscapes. Journal of Archaeological Science 2006; 33: 405-413.

[25] Higuchi T. The Visual and Spatial Structure of Landscapes. MIT Press, Cambridge, Massachusetts; 1983.

[26] Ministerio de Fomento, Spanish Government, On line: http://www.fomento.es/MFOM/LANG_CASTELLANO/DIRECCIONES_GENERALES/CARRETERAS/TRAFICO_VELOCIDADES/MAPAS/